Leins, J.A., **Banitz, T.**, **Grimm, V.**, **Drechsler, M.** (2021):
High-resolution PVA along large environmental gradients to model the combined effects of climate change and land use timing: lessons from the large marsh grasshopper
Ecol. Model. **440** , art. 109355

http://dx.doi.org/10.1016/j.ecolmodel.2020.109355

High-resolution PVA along large environmental gradients to model the combined effects of climate change and land use timing: lessons from the large marsh grasshopper

Johannes A. Leins[a,*], Thomas Banitz[a], Volker Grimm[a,b], Martin Drechsler[a,c]

[a]Helmholtz Centre for Environmental Research – UFZ, Department of Ecological Modelling, Permoserstr. 15, 04318 Leipzig, Germany
[b]Plant Ecology and Nature Conservation, University of Potsdam, Am Mühlenberg 3, 14476 Potsdam, Germany
[c]Brandenburg University of Technology Cottbus-Senftenberg, Platz der Deutschen Einheit 1, 03046 Cottbus, Germany
*corresponding author (johannes.leins@ufz.de, +49 341 235-1707)

Abstract

Both climate change and land use regimes affect the viability of populations, but they are often studied separately. Moreover, population viability analyses (PVAs) often ignore the effects of large environmental gradients and use temporal resolutions that are too coarse to take into account that different stages of a population's life cycle may be affected differently by climate change. Here, we present the High-resolution Large Environmental Gradient (HiLEG) model and apply it in a PVA with daily resolution based on daily climate projections for Northwest Germany. We used the large marsh grasshopper (LMG) as the target species and investigated (1) the effects of climate change on the viability and spatial distribution of the species, (2) the influence of the timing of grassland mowing on the species and (3) the interaction between the effects of climate change and grassland mowing. The stage- and cohort-based model was run for the spatially differentiated environmental conditions temperature and soil moisture across the whole study region. We implemented three climate change scenarios and analyzed the population dynamics for four consecutive 20-year periods. Climate change alone would lead to an expansion of the regions suitable for the LMG, as warming accelerates development and due to reduced drought stress. However, in combination with land use, the timing of mowing was crucial, as this disturbance causes a high mortality rate in the aboveground life stages. Assuming the same date of mowing throughout the region, the impact on viability varied greatly between regions due to the different climate conditions. The regional negative effects of the mowing date can be divided into five phases: (1) In early spring, the populations were largely unaffected in all the regions; (2) between late spring and early summer, they were severely affected only in warm regions; (3) in summer, all the populations were severely affected so that they could hardly survive; (4) between late summer and early autumn, they were severely affected in cold regions; and (5) in autumn, the populations were equally affected across all regions. The duration and start of each phase differed slightly depending on the climate change scenario and simulation period, but overall, they showed the same pattern. Our model can be used to identify regions of concern and devise management recommendations. The model can be adapted to the life cycle of different target species, climate projections and disturbance regimes. We show with our adaption of the HiLEG model that high-resolution PVAs and applications on large environmental gradients can be reconciled to develop conservation strategies capable of dealing with multiple stressors.

Highlights:

- Explore spatial viability of terrestrial species given dynamic external drivers
- High-resolution climate data are coupled to a demographic locust population model
- Climate change alone would benefit the locust in Northwest Germany
- Climate and land use interact nontrivially thus timing of mowing gets crucial
- Smart conservation planning should adapt mowing schedule to locally varying climate

Key words: climate change, land use, population viability analysis, stage-based model, high resolution, environmental gradients

1 Introduction

In terrestrial ecosystems, land use and climate change are two dominant factors driving biodiversity loss (Millennium Ecosystem Assessment, 2005). The risk of species loss can be estimated using simulation models that support population viability analysis (PVA) in changing environments. PVAs are used to assess the viability of species and populations as a function of species parameters such as the population growth rate, environmental conditions such as food availability and anthropogenic impacts such as the fragmentation and deterioration of habitats (Beissinger and McCullough, 2002; Coulson et al., 2001). These analyses are of great value in conservation biology to decide where, when and how which species should be protected.

While PVAs are widely performed (Chaudhary and Oli, 2020; Pe’er et al., 2013; Stephens, 2016), most of them address small areas, build on aggregated demographic rates and use low temporal resolutions (e.g., years). In recent years, however, it has become increasingly clear that three interrelated factors need to be considered in PVAs to broaden their scope. First, a large spatial extent can be important to capture relevant environmental gradients. Second, considering all life stages, i.e., the full life cycle of a species is relevant (Radchuk et al., 2013) because stages respond in different (Levy et al., 2015) or even contrary ways (Cordes et al., 2020) to changes in the environment caused, for example, by climate change. Third, the high temporal resolution of climate data has proven relevant for improving modeling results (Radchuk et al., 2014), for instance, to capture the impact of extreme conditions (Ma et al., 2015). The second and third factors are interrelated, as capturing the response of different life stages to external conditions requires high-resolution data. Yet, to our knowledge, only few studies so far use such highly resolved external drivers, especially in combination with spatial gradients and distinguishing different life stages (Bonnot, 2016; Green et al., 2014; Schmidt and Zinkernagel, 2017; Thompson et al., 2012).

Here, we present the *Hi*gh-resolution *L*arge *E*nvironmental *G*radient (HiLEG) model, a spatially differentiated stage- and cohort-based simulation model that allows us to use daily time steps, to mechanistically examine the interrelations between population dynamics and external drivers, such as climate and land use. The HiLEG model is designed to be used for different terrestrial animal species by specifying a corresponding set of parameters and external drivers along large environmental gradients.

We use climate data with a daily temporal resolution and a spatial resolution of 12 x 12 km² grid cells and that widely cover Northwest Germany. In each climate cell, a representative patch of grassland is considered. Similar to a sensitivity analysis, the comparison of the model results for different climate cells allows the exploration of the dependence of population viability on climate change and land use as well as the interaction between the two factors.

Experimental data on the impact of climate parameters such as temperature, precipitation and soil moisture on population dynamics are usually scarce and uncertain, which is also the case in the present study. The output of the model simulations is thus too uncertain to make quantitative predictions on the future development or viability of a target species. However, relative predictions and comparative analyses are usually robust to data uncertainty (Drechsler et al., 2003; McCarthy and Possingham, 2014), for example, if they address the influence of an environmental factor on the ranking of habitats or land use measures with regard to their suitability for a species. The present PVA is such a relative analysis.

As a first application, we parametrized the HiLEG model for the well-studied large marsh grasshopper (LMG, *Stethophyma grossum*) in cultivated grasslands of Northwest Germany and simulated its population dynamics for the years 2000-2079, given different climate change scenarios and schedules for grassland mowing. The LMG prefers wet meadows and marshes as habitats, while its life stages are affected differently by climate conditions and the timing of grassland mowing: Warm temperatures accelerate hatching and larva development while spring and autumn droughts degrade eggs located below ground. Mowing is highly lethal for larvae and imagines because they can hardly escape the harvesters. The LMG is partly considered threatened in the federal states of Northwest Germany (Winkler, 2000) and therefore of high relevance for local conservation agencies. While recent studies project this species will benefit from elevated temperatures caused by climate change (Poniatowski et al., 2018; Trautner and Hermann, 2008), they state that extended droughts and anthropogenic disturbances such as mowing and grazing – depending on their timing – can still pose a threat to its survival (Löffler et al., 2019; Poniatowski et al., 2018).

Our model allows simulating the combined effects of different scenarios of climate change and mowing schedules on LMG population dynamics. Therefore, it helps to evaluate possible conservation measures by assessing how the timing of grassland mowing can be altered to adapt to climate-induced shifts in the LMG life cycle. To this end, the model considers temporal changes and spatial heterogeneity in essential climate variables. In principle, our model is also able to consider spatial heterogeneity in other factors, such as habitat size, food competitors, predators and land use. However, the aim of the model is not to investigate real land use patterns with spatially heterogeneous mowing dates or other heterogeneous features in the study region. Rather, our model aims to solve the problem of coupling high-resolution climate data into a demographic model and investigating how the dynamics of local LMG populations are affected by the locally changing climate and selected mowing schedules. Specifically, the following questions are addressed: (1) How do population density and viability shift regionally, given different climate change scenarios? (2) Which mowing schedule has the least negative impact on the overall population density and viability in the study region? (3) Does the mowing impact severity depend on the spatial location (with its specific climate)?

2 Material and methods

Our case study involves four main components: the study region (Northwest Germany and the surrounding areas), the target species (LMG), climate data (projections until 2080) and land use (grassland mowing). These components are described in the following subsections. Furthermore, the HiLEG model, which simulates the interplay between these components, is introduced in subsection 2.6.

2.1 Study region

The study region is Northwest Germany and the surrounding areas (Figure 1), for which climate projections were available (section 2.3). More precisely, those regions are the federal states of Schleswig-Holstein, Lower Saxony, Hamburg and Bremen as well as surrounding areas of Germany, Denmark and the Netherlands. The spatial resolution of the grid cells areas of 12 x 12 km^2 yields 968 terrestrial grid cells within the study region.

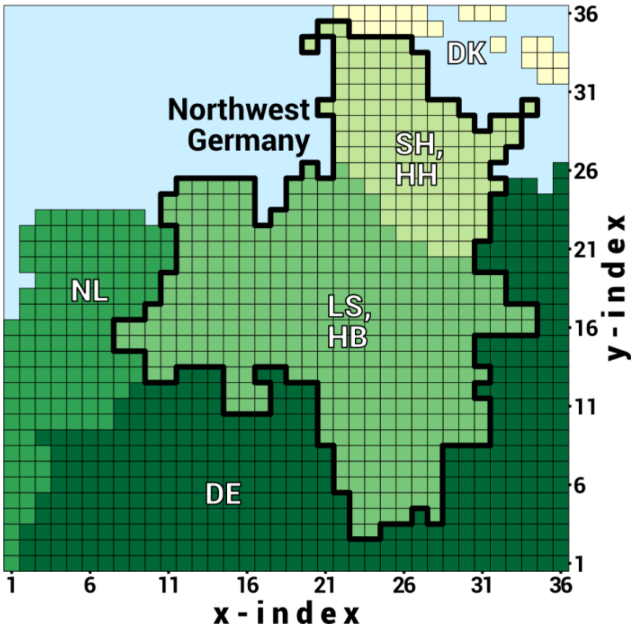

Figure 1: Spatial representation of the study region and its subareas. Each terrestrial grid cell (shades of green and yellow) has an area of 12 x 12 km^2. Northwest Germany is highlighted by a thick black outline. Abbreviations: DE=Germany, DK=Denmark, HB=Bremen, HH=Hamburg, LS=Lower Saxony, NL=the Netherlands, SH=Schleswig-Holstein. The blue areas show the North and Baltic Seas.

2.2 Target species

The LMG (*S. grossum*) (Linné 1758) is a well-studied locust species that is widely distributed in Central European grass- and wetlands (Heydenreich, 1999). Though the grasshopper itself tolerates a wide range of temperatures and humidity, the high water demand of its eggs restricts the LMG to wet habitats such as meadows and marshes (Ingrisch and Köhler, 1998; Koschuh, 2004). During a year, it develops through three consecutive life stages (Figure 2), which often overlap to some degree within a population: (1) egg/embryo, typical timing between July and June of the following year, below ground; (2) larval, May-October, above ground; (3) imago, July-October, above ground; (Heydenreich, 1999; Ingrisch and Köhler, 1998; Kleukers et al., 1997; Köhler and Weipert, 1991; Malkus, 1997; Marshall and Haes, 1988; Oschmann, 1969). Stage 1 goes through additional development phases that are included in our model: The embryo development inside the egg is interrupted by a diapause to prevent too early development under rather good conditions, and an extended cold period is needed to break this diapause. Furthermore, for ideal development, the eggs need to be exposed to *contact water* before and after winter (Ingrisch, 1983), i.e., they must be covered with water or lie in moist soil.

Similar to other locusts, the LMG is regarded as an indicator for the quality of grassland habitats (Báldi and Kisbenedek, 1997; Heydenreich, 1999; Keller et al., 2012; Keßler et al., 2012). It is considered threatened in parts of the study region, e.g., according to the red lists for Schleswig-

Holstein (Winkler, 2000) and Germany (Blab et al., 1984; Maas et al., 2002). To our knowledge, more recent lists are not available.

The climate conditions within the LMG's habitat have different implications for population development. Warm temperatures accelerate embryo hatching in spring (Wingerden et al., 1991) and larval development during summer (Ingrisch and Köhler, 1998; Uvarov, 1977). A sustained dry upper soil layer (depth of 2-10 cm) before and after winter causes drought stress during egg/embryo development (Ingrisch, 1983). Considering both factors in terms of climate change, there are two implications for the LMG. On the one hand, increasing temperatures might be beneficial because the accelerated species development could lead to larger population densities and therefore promote dispersal to new habitats (Poniatowski et al., 2018; Trautner and Hermann, 2008). On the other hand, extended droughts could threaten hygrophilous species like the LMG (Löffler et al., 2019), especially if they occur during spring or autumn, by inhibiting egg and embryo development.

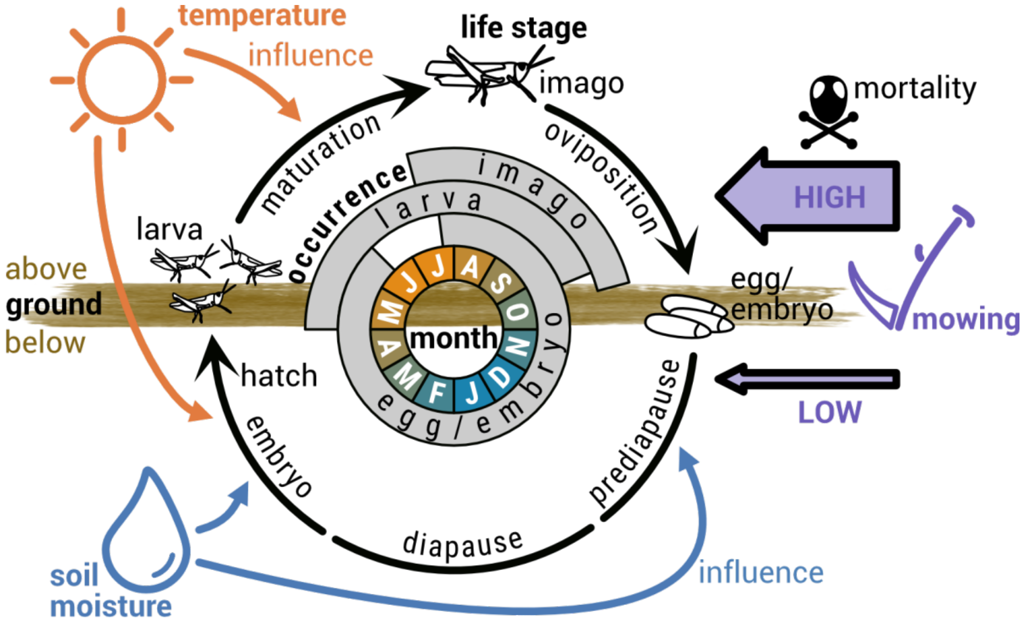

Figure 2: Yearly life cycle of the LMG, including the influence of external drivers. Black life stage symbols and circular arrows represent processes between and during life stages, where the life stage egg/embryo is subdivided into three phases (broken arrow). The typical ranges of the life stage occurrences are indicated in gray. The inner circle depicts months, where the color indicates seasonal changes in temperature. The influence of the external drivers of temperature, soil moisture and mowing is shown by colored symbols and arrows. Mowing impact is distinguished into high (aboveground) and low (belowground) mortality.

Mowing is particularly harmful during the aboveground phase, as larvae and imagines can hardly escape the harvesters and are mostly killed (Malkus, 1997; Marzelli, 1997). Eggs and embryos, however, are only mildly affected by the mechanical soil disturbances of harvesters. Therefore, extensive grassland mowing with 1-2 cuts during the belowground phase, i.e., early or late in the year, is not considered problematic. It can even benefit the LMG by maintaining the grasshopper's favored microclimate in an open and heterogeneous vegetation structure (Malkus, 1997; Miller and

Gardiner, 2018; Sonneck et al., 2008). To limit complexity, other factors of grassland suitability, such as vegetation structure or food availability, are not included in this study and are instead considered ideal for LMG development.

2.3 Climate data

The climate data are taken from high-resolution scenario simulations generated by the regional climate model COSMO-CLM[1] (CCLM4-8-17) introduced by Keuler et al. (2016). For our study, this regional model was driven at its lateral boundaries by simulation results of the global model ICHEC[2]-EC-EARTH and three Representative Concentration Pathways (RCPs): RCP2.6, RCP4.5 and RCP8.5. These pathways represent potential climate developments with different global warming rates for the 21st century. The number indicates the equivalent of additional radiative forcing in W m^{-2} (van Vuuren et al., 2011) of the increasing greenhouse gas concentrations by the year 2100. Hereafter, the climate change scenarios will be distinguished by action taken towards reducing CO_2 emissions: *full force* (*FF*, RCP2.6), *moderate* (*MOD*, RCP4.5) and *business as usual* (*BAU*, RCP8.5). The regional model provides time series of daily climate data values (mean or sum) that are spatially resolved to grid cells of size 12 x 12 km^2. Common in such regional models, these cells are located in a rotated pole grid coordinate system. COSMO-CLM only provides a single climate projection per global model, RCP and grid cell that would have limited HiLEG to deterministic time series within a climate change scenario. To mitigate this limitation for the stochastic model processes (section 2.5), we resampled the climate time series per replicate run by randomly rearranging the years without losing the long-term trend (see Supplements S2 and S4, section 5). From the available data, we used time series for the years 1995-2080, with the regional model providing simulated data from 2006 onwards. Only the data before 2006 are readings of actual meteorological values.

We considered three climate parameters relevant for the LMG population dynamics as implemented in our model: *surface temperature (ts)* [°C]*, contact water (cw)* [kg m^{-2}] and *relative humidity-upper ground (rhug)* [%]. Parameter *ts* is explicitly calculated by the climate model described below and simply referred to as *temperature* hereafter. The parameters *cw* and *rhug* are deduced from other provided time series (see Supplement S1). They were established because a sufficient amount of contact water and humidity in the upper soil layer is relevant for the LMG egg development, as described by Ingrisch (1983). Throughout the model, *cw* and *rhug* are used in combination and are therefore referred to by the joint term *humidity* hereafter.

Additionally, we introduced the parameter *relative soil moisture content (rsmc)* [%], hereafter referred to as *soil moisture*. It is a representation of the parameter *total soil moisture content (mrso)*

---

[1] Consortium for Small-scale Modeling in Climate Mode

[2] Irish Centre for High-End Computing

[kg m^{-2}] calculated by the climate model divided by its yearly maximum values. *Soil moisture* and *humidity* are correlated parameters, as both depend on *mrso* (see Supplement S1, equations S1-2, S1-7 and S1-10). In our analysis, we mainly focus on *soil moisture* for reasons of simplicity. It is closer to parameters considered by stake holders (e.g., total soil moisture, precipitation) than the more abstract parameter *humidity* (in terms of our model) and is thus easier to comprehend. Together with the parameter *temperature*, projections of *soil moisture* for the years 2000-2080 are given in Figure 3. Their spatial distributions in the study region are shown in Figure 5.

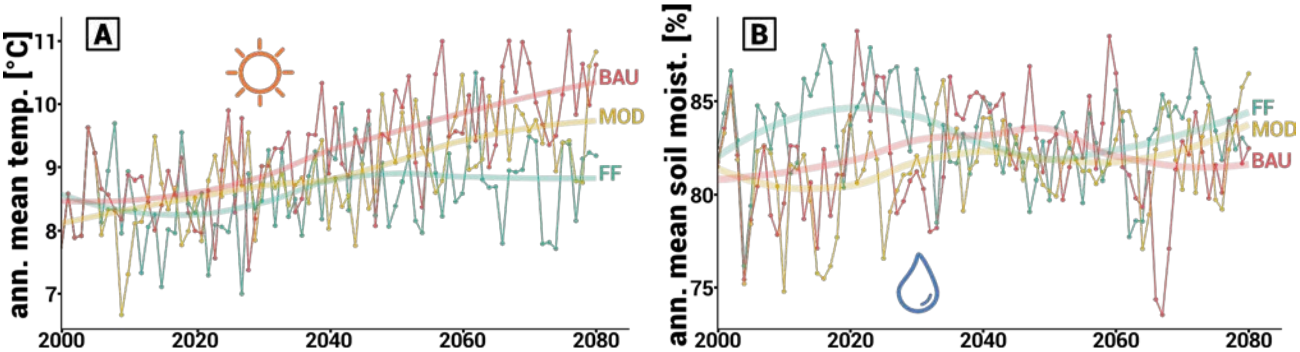

Figure 3: Projections of the annual mean values for the climate parameters *temperature* (A) and *soil moisture* (B) for the years 2000-2080. Climate change scenarios *FF*, *MOD* and *BAU* are indicated by colors (and labels). The thin lines show the actual means of the parameter values; the thick lines show the smoothed trends.

2.4 Land use

Anthropogenic influence on the model species is represented by mechanical mowing as a scheduled grassland use measure. It is executed uniformly over the whole study region once per year at the beginning of the same calendar week (mowing day). Within our model, mowing has a solely negative effect on the model species, but with different severities for the below- and aboveground populations. Other indirect effects of mowing are not included in the model (see section 2.2).

2.5 Simulation output

For each simulation scenario, we generated fifty replicate runs (using different random seeds) to account for stochasticity (section 2.6, Table 3). To assess and compare the suitability of different regions for population viability under different scenarios, we focused on two output values per grid cell: the mean population density (referred to as ‘mean density’ hereafter) over the full simulation duration and all replicates and the mean population lifetime (referred to as ‘mean lifetime’ hereafter) over all replicates.

Note that the maximum duration of simulation runs limits the lifetime to 20 years in our analysis. Values close to 20 years hint at population survival over the whole simulation duration in most (or all) replicates, and, thus, hint at good conditions for longer persistence as well.

2.6 Model description

A full model description following the ODD (Overview, Design concepts, Details) protocol (Grimm et al., 2020, 2006) is provided in Supplement S4. Here, we provide a 'Summary ODD' (Grimm et al., 2020), which includes the models' overall rationale, an overview of the entities and processes, and verbal descriptions of the key processes. In the following, ODD keywords are in italics and capitals.

The HiLEG model is applied to the life cycle of the LMG, whose life stages are affected by climate and land use. Climate conditions affect development and mortality, while land use (mowing events) induces additional mortality, especially during the aboveground phase. By its present parameterization, the model is nonspatial in the sense that the local LMG populations do not interact with each other. Spatial heterogeneity in land use and biotic variables such as habitat size are ignored. However, the essential climate variables are spatially differentiated to apply the model to spatial gradients in climate change scenarios, covering Northwest Germany and the surrounding regions (Figure 1). The *PURPOSE* of the model is to answer the following questions: (1) How do the population density and lifetime shift regionally, given different climate change scenarios? (2) Which mowing schedule has the least negative impact on the overall population density and viability in the study region? (3) Does the mowing impact severity depend on the spatial location (with its specific climate)?

The empirical *PATTERNS* used to ensure that the model is sufficiently realistic for its purpose are the observed features of the life cycle and their sensitivity to environmental conditions, which were taken from the literature. These patterns were used for the model's design. The model output in terms of the population structures, densities and persistence were not compared to other data, as such data are sparse. Therefore, all model predictions are relative, not absolute. The model was implemented in C++. The source code of the model implementation, the executable program and the input files used for the simulations runs are available via a GitLab repository[3].

The model has the following *ENTITIES*: *Grid Cells* (defining environmental conditions), and *Population* per grid cell comprised of *Life Stages,* which are comprised of age-distinguished *Cohorts*. *Flows* are auxiliary entities that manage the density transfer between *Life Stages* or their loss through mortality. Table 1 provides an overview of the model's entities and their *STATE VARIABLES*. The LMG develops through three main *Life Stages* during a year (section 2.2). Following Ingrisch (1983) and Wingerden et al. (1991), we divided the egg/embryo stage into prediapause, diapause and postdiapause development (called 'embryo' hereafter) to account for the clutch's different susceptibility to climate conditions in autumn, winter and spring.

---

[3] HiLEG GitLab repository: https://git.ufz.de/leins/hileg

This subdivision yields five *Life Stages*: (1) prediapause, (2) diapause, (3) embryo, (4) larva, and (5) imago. Stages 1 to 3 occur below ground, and stages 4 and 5 occur above ground. Furthermore, stages 2 and 4 can have multiple *Cohorts* to account for survival over several years in case of conditions during winter that are unsuitable for development and to account for different temperature-driven development speeds depending on the hatching date.

Table 1: Overview of the model's entities (first column) and their state variables (second column). The text in parentheses of columns one and two represents the entity's or state variable's symbol when used, e.g., in equations. The third column gives the (initial) value(s) of the state variables, the fourth column gives their units (if any). In the fifth column, a brief description of the state variable is provided. The indexes for location and time step that distinguish entities and their dynamically changing states are implied and not explicitly specified in the identifier. The parameter A_{hab}=62,500 m^2 is the habitat size modeled for a population.

Entity (symbol)	State variable (symbol)	Value(s)	Unit	Description
Population (P)	coordinates ($coord_{x,y}$)	$x, y \in [1,36]$		Index of rotated pole grid coordinates (see the main text)
	set of life stages (P^{stages})	$\{S^{pre}, S^{dia}, S^{emb}, S^{lar}, S^{ima}\}$		Distinguished life stages of the target species
	density ($dens^P$)	$\sum\{dens^{pre}, dens^{dia}, dens^{emb}, dens^{lar}, dens^{ima}\}$	ind. m^{-2}	Summed life stage densities
	aboveground density ($dens^P_{above}$)	$\sum\{dens^{lar}, dens^{ima}\}$	ind. m^{-2}	Summed density of the aboveground life stages
	minimum density ($dens_{min}$)	$1/A_{hab}$	ind. m^{-2}	Minimum of one individual per habit
Life Stage (S^{name})	name	$\in \{pre, dia, emb, lar, ima\}$		Name of the distinguished life stages
	set of cohorts ($S^{name}_{cohorts}$)	$\{C^m, .., C^n\}$, $\{m, n\} \in N$		Distinguished cohorts associated with the life stage
	density ($dens^{name}$)	$\sum\{dens^m, .., dens^n\}$,$\{m, n\} \in N$	ind. m^{-2}	Summed densities of the associated cohorts
	gain ($gain^{name}$)		ind. m^{-2}	Summed total flow amount of the incoming flows (see below)
	aboveground flag ($above^{name}$)	$\in \{TRUE, FALSE\}$		Boolean flag defining whether the stage occurs above ground
	maximum age (age^{name}_{max})	$\in \{210,1700,120,90,120\}$	days	Maximum age of the associated cohorts
Cohort (C^{ID})	ID	$\in N$		Unique cohort identifier
	density ($dens^{ID}$)		ind. m^{-2}	The cohort's individual density
	age (age^{ID})		days	Age in days since cohort creation
	development progress ($prog^{name}_{ID}$)	$\in [0,1]$		The ratio of development compared to full development
	developing flag (dev^{ID})	$\in \{TRUE, FALSE\}$		Boolean flag defining the use of $prog^{ID}$ (see the main text)
Flow (F^{name}_{type})	type (*type*)	$\in \{trans, repr, mort\}$		Defines how the flow is processed
	life stage of origin ($orig$)	$\in \{S^{pre}, S^{dia}, S^{emb}, S^{lar}, S^{ima}\}$		Life stage used to determine the amount of flow
	life stage of destination ($dest$)	$\begin{cases} mort & if type = mort \\ \in \{S^{pre}, S^{dia}, S^{emb}, S^{lar}, S^{ima}\} & otherwise \end{cases}$		Life stage receiving the amount of flow, or the amount of mortality
	set of influences (I^{name}_{type})			Environmental drivers associated with this flow
	base flow rate ($rate^{name}_{type}$)		day^{-1}	Daily per capita base flow rate
	dynamic flow rate (dyn^{ID}_{type})		day^{-1}	Daily per capita flow rate per cohort in the life stage of origin
	current flow amount ($amount^{ID}_{type}$)	$dens^{ID} \times dyn^{ID}_{type} \times day$	ind. m^{-2}	Amount of density flow over one day
	total flow amount ($amount^{name}_{type}$)	$\sum\{amount^m_{type}, .., amount^n_{type}\}$, $\{m, n\} \in N$	ind. m^{-2}	Summed amount (per cohort) of density flow over one day
Grid Cell (G)	coordinate ($coord_{x,y}$)	$x, y \in [1,36]$		Index of rotated pole grid coordinates (see main text)
	carrying capacity (cap_{above})	25	ind. m^{-2}	Maximum aboveground density
	temperature (ω_{ts})		°C	Local surface temperature
	humidity (ω_{rhug})		%	Local relative humidity in the upper 2 cm of the ground
	contact water (ω_{cw})		kg m^{-2}	Amount of water in the upper 2 cm of the ground
	mowing day (t_{mow})	none or $\in \{134,141,..,274\}$	day	Day of yearly mowing event

Abbreviations: above=aboveground, C=*Cohort*, cap=capacity, coord=coordinate, cw=contact water, dens=density, dest=destination, dev=development, dia=diapause, dyn=dynamic, emb=embryo, F=*Flow*, G=*Grid Cell*, hab=habitat, ID=*Cohort* identifier, ima=imago, ind=individuals, kg=kilogram, lar=larva, m=meter, max=maximum, min=minimum, mort=mortality, mow=mowing, orig=origin, P=*Population*, pre=prediapause, prog=progress, repr=reproduction, rhug=relative humidity upper ground, S=*Life Stage*, t=time step, temp=temperature, trans=transfer

The transition between different *Life Stages* is complex because the development and/or mortality of *Cohorts* and *Life Stages* depends on their previous state and is influenced by climate conditions (*temperature*, *humidity*). *Flows* are therefore used to collect all the contributions of all the *Cohorts* of a certain *Life Stage* that completed development and therefore 'flow' to the next *Life Stage*. In the case of mortality, a *Flow* determines the amount of density lost by a *Life Stage* and its *Cohorts*.

The model uses daily time steps. Here, *SCALE* also reflects the sampling of the climate data. However, the single mowing event per year is considered on a weekly basis (the first day of a calendar week). To account for this weekly frequency, a year has 364 days by definition, resulting in exactly 52 full calendar weeks. Simulations were run for 20 years (7280 time steps) or stopped earlier for a local *Population* in the case of extinction.

The study region comprises 1296 (36 x 36) grid cells, each having an area of 144 km² (12 km x 12 km), which corresponds to the resolution of the climate input data (Figure 1). In total, 968 grid cells are terrestrial and therefore belong to the model domain. Within a grid cell, a single habitat is considered, which represents a virtual grassland plot with a size of 6.25 ha (250 m x 250 m). Grid cells and hence habitats are not connected; i.e., there is no exchange of individuals: if populations become extinct, there is no recolonization.

The model is *INITIALIZED* with a starting date, simulated duration, mowing day and climate change scenario (Table 2). Additionally, each *Population* receives an initial density per *Life Stage* (i.e., 1000 eggs in the diapause stage, zero density for the other *Life Stages*). The *carrying capacity* [individuals m^{-2}] for the aboveground population (i.e., the larva and imago *Life Stages* only) is assumed to be identical for all the *Grid Cells* to reduce the number of confounding factors in the model analysis. We used the four 20-year time intervals 2000-2019 (abbreviated to 2000-19 hereafter), 2020-39, 2040-59 and 2060-79 to track changes for past and future climate conditions. Time series of climate data per grid cell are used as *INPUT DATA*, which drives the model's dynamics.

Table 2: List of variables used to initialize a simulation run. The first column is the variable name used in the text. The second column is the variable symbol when used in the model equations. The third column is the initial value(s)/value options used for the simulation runs. The fourth column is a brief description of the variable. The parameters below the double line can vary in principle but are constants in the presented work.

Variable Name	**Symbol**	**Value(s)**	**Description**
starting date	t_{init}	1st Jan. 2000, 2020, 2040, 2060	The date of initial time steps translated to climate data index
mowing day	t_{mow}	none or day 134, 141,…,274	The timing of mowing per year
climate change scenario	CCS	FF, MOD or BAU	Representative Concentration Pathways of CO_2 model
duration	t_{Δ}	7280 days	Runtime in days
habitat area	A_{hab}	250 x 250 m^2	Area of grassland plot inside a grid cell
initial density	$dens_{init}$	$\{0,1000,0,0,0\}/A_{hab}$	The initial population density per life stage in individuals m^{-2}
carrying capacity	cap_{above}	25 individuals m^{-2}	maximum aboveground density per square meter

Abbreviations: FF=full force, MOD=moderate, BAU=business as usual, above=aboveground, cap=capacity, dens=density, hab=habitat, init=initial, mow=mowing, scen=scenario, t=time step

Table 3 provides an overview of the model's *PROCESSES*. Each *Life Stage* has its own set of processes. The basic rationale of the model is to assume a daily base rate for all processes, which represents benign or observed average environmental conditions. This base rate is then modified ('influenced') by environmental drivers. Our model includes predefined functions or equations – called *Influences* – that may be applied under certain environmental conditions. The equations used to represent the *Influences* and their parameterization as applied to the target species are listed in Supplement S4, Tables S4-4 and S4-5. Generally, each *Influence* provides a factor that can mediate the effect of environmental conditions on the variables *dynamic flow rate* and *development progress* of a *Flow* or *Cohort*, respectively.

Table 3: Overview of the model processes and their daily rates and equations. Processes (second column) are distinguished by *Life Stage* (first column) and referenced by their symbol (third column) as used in the model equations. The fourth column defines the equation and environmental drivers (*Influences*, bold f-symbols, cf. Table S4-4 of Supplement S4) used for calculating a cohort-specific dynamic rate. Equation segments marked with *s are simplifications of the iterative process of updating the flow rate described in Pseudocode S4-3 of Supplement S4. Superscript letters reference the sources used to parameterize the processes and equations for the LMG (coefficients in Table S4-5 of Supplement S4): [a] Ingrisch (1983), [b] B. Schulz (pers. comm.), [c] Wingerden et al. (1991), [d] Ingrisch and Köhler (1998), [e] Helfter and Sänger (1975), [f] Helfert (1980), [g] Kriegbaum (1988), [h] Waloff (1950).

Life stage (symbol)	Process	Process symbol	Dynamic rate (daily)	Description
pre-diapause (S^{pre})	mortality	F_{mort}^{pre}	$dyn_{mort}^{ID} = rate_{mort}^{pre} + (1 - rate_{mort}^{pre})^{*} \times \left[f_{sig}^{A} \times f_{thd}^{B} + f_{mow}^{C}\right]$	The base mortality rate [a] increases in two cases: (1) humidity-driven (f_{sig}^{A}) [a] if contact water (f_{thd}^{B}) [a] is missing; (2) if mowing is scheduled (f_{mow}^{C}) [b]
	development	$prog_{ID}^{pre}$	$prog_{ID}^{pre} = \begin{cases} prog_{ID}^{pre} + f_{thd}^{D} & if\, f_{thd}^{D} > 0 \\ 0 & otherwise \end{cases}$	Needs three days below 10 °C in a row (f_{thd}^{D}) [a] to fully develop
	transfer	F_{trans}^{pre}	$dyn_{trans}^{ID} = \begin{cases} 1 & if\, prog_{ID}^{pre} = 1 \\ 0 & otherwise \end{cases}$	Immediately transfers to diapause stage if fully developed
diapause (S^{dia})	mortality	F_{mort}^{dia}	$dyn_{mort}^{ID} = rate_{mort}^{dia} + \left(1 - rate_{mort}^{dia}\right) \times f_{mow}^{E}$	The base mortality rate increases if mowing is scheduled (f_{mow}^{E}) [b]
	development	$prog_{ID}^{dia}$	$prog_{ID}^{dia} = \begin{cases} prog_{ID}^{dia} + f_{thd}^{F}/2 & if\, prog_{ID}^{dia} < 0.5 \\ prog_{ID}^{dia} + f_{thd}^{G}/2 & if\, prog_{ID}^{dia} \geq 0.5 \wedge f_{thd}^{G} \neq 0 \\ 0.5 & otherwise \end{cases}$	Needs 61 days below 5 °C to break diapause (f_{thd}^{F}) [a,c] and afterwards three days above 10 °C in a row (f_{thd}^{G}) [a] to fully develop. Temperatures > 5 °C before diapause is broken reverse development
	transfer	F_{trans}^{pre}	$dyn_{trans}^{ID} = \begin{cases} 1 & if\, prog_{ID}^{dia} = 1 \\ 0 & otherwise \end{cases}$	Immediately transfers to embryo stage if fully developed
embryo (S^{emb})	mortality	F_{mort}^{emb}	$dyn_{mort}^{ID} = rate_{mort}^{emb} + (1 - rate_{mort}^{emb})^{*} \times \left[f_{exp}^{H} + f_{sig}^{I} \times f_{thd}^{J} + f_{mow}^{K}\right]$	The base mortality is defined by the temperature (f_{exp}^{H}) [c]. It increases in two cases: (1) humidity (f_{sig}^{I}) [a] if contact water (f_{thd}^{J}) [a] is missing and/or (2) if mowing is scheduled (f_{mow}^{K}) [b]
	transfer	F_{trans}^{emb}	$dyn_{trans}^{ID} = rate_{trans}^{emb} \times f_{bin}^{L}\left(f_{exp}^{M}, f_{exp}^{N}, dens^{ID}, prog_{ID}^{name}\right)$	The base transfer rate is multiplied by a temperature- (f_{exp}^{M}, f_{exp}^{N}) [c], progress- and the density-driven hatching probability stemming from a binomial distribution (f_{bin}^{L})
larva (S^{lar})	mortality	F_{mort}^{lar}	$\mathrm{dyn}_{\mathrm{mort}}^{\mathrm{ID}} = \mathrm{rate}_{\mathrm{mort}}^{\mathrm{lar}} + \left(1 - \mathrm{rate}_{\mathrm{mort}}^{\mathrm{lar}}\right)^{*} \times \left[f_{cap}^{O} + f_{lin}^{P} + f_{mow}^{Q}\right]$	The base mortality rate [d] increases with density (f_{cap}^{O}) [b] and in two additional cases: (1) the temperature (f_{lin}^{P}) is below 10 °C and/or (2) if mowing is scheduled (f_{mow}^{Q}) [b]
	transfer	F_{trans}^{lar}	$\mathrm{dyn}_{\mathrm{trans}}^{\mathrm{ID}} = \mathrm{rate}_{\mathrm{trans}}^{\mathrm{lar}} \times f_{bin}^{R}\left(f_{lin}^{S}, f_{lin}^{T}, \mathrm{dens}^{\mathrm{ID}}, \mathrm{prog}_{\mathrm{ID}}^{\mathrm{lar}}\right)$	The base transfer rate is multiplied by a temperature- (f_{lin}^{S}, f_{lin}^{T}) [e,f], progress- and density-driven maturation probability stemming from a binomial distribution (f_{bin}^{R})
imago (S^{ima})	mortality	F_{mort}^{ima}	$\mathrm{dyn}_{\mathrm{mort}}^{\mathrm{ID}} = \mathrm{rate}_{\mathrm{mort}}^{\mathrm{ima}} + \left(1 - \mathrm{rate}_{\mathrm{mort}}^{\mathrm{ima}}\right)^{*} \times \left[f_{cap}^{U} + f_{lin}^{V} + f_{mow}^{W}\right]$	The base mortality rate [g] increases with density (f_{cap}^{U}) [b] and in two additional cases: (1) the temperature (f_{lin}^{V}) is below 10 °C and/or (2) if mowing is scheduled (f_{mow}^{W}) [b]
	reproduction	F_{repr}^{ima}	$\mathrm{dyn}_{\mathrm{repr}}^{\mathrm{ID}} = \mathrm{rate}_{\mathrm{repr}}^{\mathrm{ima}}$	Fixed reproduction rate [d,h]

Abbreviations: bin=binominal, cap=capacity, dens=density, dia=diapause, emb=embryo, exp=exponential, f=symbol of Influence function, F=*Flow*, ID=*Cohort* identifier, ima=imago, lar=larva, lin=linear, mort=mortality, mow=mowing, pre=prediapause, prog=progress, repr=reproduction, sig=sigmoid, t=time step, thd=threshold, trans=transfer

In each time step and for every grid cell, four main blocks of *PROCESSES* are *SCHEDULED:* ‘Update environmental drivers’, ‘Flow update’, ‘Life Stage update’, and ‘Cohort update’. The first three blocks are scheduled one after the other, while ‘Cohort update’ is executed as a submodel of ‘Life Stage update’. During ‘Flow update’, the *Flow*’s state variables (Table 1), *total flow amount*, *current flow amount* and *dynamic flow rate* are calculated from the contributions of *Cohorts*’ state variables, including the effects of environmental influences. The submodel ‘Life Stage update’ then calculates a *Life Stage*’s *gain* from the incoming transfer *Flow* of its preceding *Life Stage* and its *density* from the *density* of its subordinate *Cohorts*: *gain* is used to determine whether to create a new *Cohort* from it or add it to an existing *Cohort*; densities of the subordinate *Cohorts* are determined by the submodel ‘Cohort update’ before they are added to the *Life Stage*’s density. Furthermore, *Cohorts* that exceed the maximum age before progressing to the next *Life Stage* or whose density falls below a certain minimum are removed. During ‘Cohort update’, a *Cohort*’s density is changed by adding the potential *gain* determined by the ‘Life Stage update’ submodel and subtracting loss through mortality or the outgoing transfer *Flow*. Additionally, some *Cohorts* develop only if environmental conditions are suitable, so their development progress is updated accordingly.

Figure 4 provides an overview of the model’s entities, the processes, and their interactions via *Flows* and *Influences*.

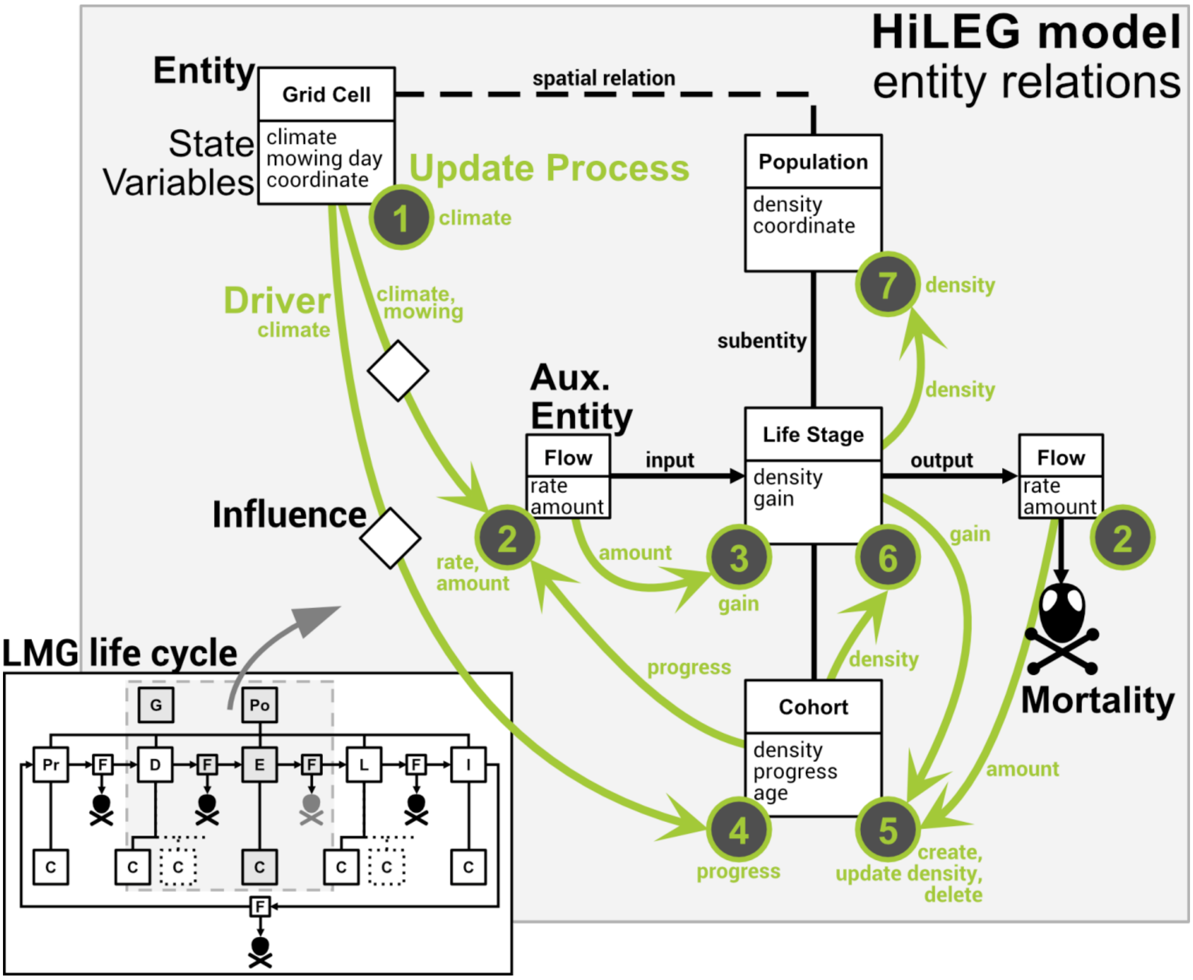

Figure 4: Overview of the model entities (boxes), their relations (black lines and arrows), and the order and drivers of the update process (green) for a single grid cell during one time step. The entities are *Grid Cell*, *Population*, *Life Stage*, *Cohort* and *Flow* (an auxiliary entity that uses state variables of the previous time step to manage the density transfer between *Life Stages* and loss through mortality). Influences define the impact of environmental conditions on model processes. The white subplot shows entities and their relations as applied to the LMG life cycle. The gray dashed rectangle within the subplot highlights entities used to explain the update process (main plot). The scheduling of the processes is as follows: (1) Update the environmental conditions. (2) Update the flow rates and amounts depending on the climate conditions and mowing while considering the development processes of the associated *Cohorts*. (3) Calculate the gain of the *Life Stage* depending on the input flow amount. (4) Update the development progress of the existing *Cohorts* depending on the climate conditions. (5) Create a new *Cohort*, and update the density of existing *Cohorts* and/or delete *Cohorts* that are of too low density or overaged depending on the *Life Stage*'s gain and output flow amount. (6) Calculate the *Life Stage* density by summing its *Cohorts'* densities. (7) Calculate the *Population* density by summing its *Life Stages'* densities. Symbols: *Entities* (squares), *Influences* (diamonds), *Processes* (circles, text corresponds to modified state variables), *Drivers* (green arrows, text corresponds to state variable used in target *Process*), optional *Cohorts* (dotted squares and lines). Abbreviations in the LMG life cycle: C=*Cohort*, D=diapause, E=embryo, F=*Flow*, G=*Grid Cell*, I=imago, L=larva, Po=*Population*, Pr=prediapause.

3 Results

The results presented here are subdivided into three sections: (1) patterns and trends found in the climate data that are relevant to the LMG (section 3.1); (2) analysis of the HiLEG model output stemming from simulations with climate as only external driver (section 3.2); and (3) analysis of the simulation runs with mowing as an additional anthropogenic impact on the LMG (section 3.3). Since the results are complex, as they cover large environmental gradients and detailed effects of environmental drivers on the study species, in the following, the main results are also directly discussed in terms of the underlying mechanism. Note that the model output occasionally reaches densities close to the population's carrying capacity, which in reality is rarely the case on a large scale. Within the idealized conditions (section 2.2) of our model realization, however, this behavior is expected and can be considered unproblematic for the analysis, because we were focusing on the relative impacts of climate change and land use on population development rather than those of density dependence.

3.1 Patterns and trends in climate data

The different climate projections showed spatial patterns and temporal trends for the years 2000 to 2079 in terms of *temperature* and *soil moisture*. Note that for reasons of consistency, even the past time period 2000-19 consists mostly of simulated data (see section 2.3). The coarse spatial patterns for all the climate change scenarios, averaged over 20-year periods, show that temperature increased slightly from north to south, except for two colder mountain regions in the south (Figure 5, marks 1-2). Over time, the temperature generally increased similarly in the study region. Overall, the increase was stronger for more severe scenarios with three exceptions. First, during the simulation period 2000-19, temperatures were more or less identical between the scenarios. Second, for the period 2020-39, the temperature increase was slightly higher for scenario *MOD* than for *BAU*. Third, during the late periods 2040-59 and 2060-79, temperature remained almost constant for scenario *FF*.

For soil moisture, the patterns were more complex than those of temperature. There were four regions of distinctively low soil moisture (Figure 5, marks 3-6) because these regions have a soil type that seems to favor drought (K. Keuler, *pers. comm.*, cf. Keuler et al., 2016). During the first period (2000-19), the *MOD* and *BAU* scenarios clearly showed lower soil moisture than the *FF* scenario in almost all the cells and an additional dry region in the southeast (Figure 5, mark 6). Over time, however, many of those cells improved for the severe *BAU* scenario while degrading for the *FF* scenario. Nonetheless, the soil moisture for the *BAU* scenario was barely higher than that for the intermediate *MOD* scenario (Figure 3).

Overall, the spatial patterns in the soil moisture showed the following temporal trends: The northwestern dry region expanded over time (Figure 5, mark 4); some small dry regions appeared in the center of the study region; the moisture of the mountain regions increased less than that of their surroundings; the edges around the central eastern dry region became wetter; and there was a spatial gradient of soil moisture increase in the southeast and decrease in the northwest.

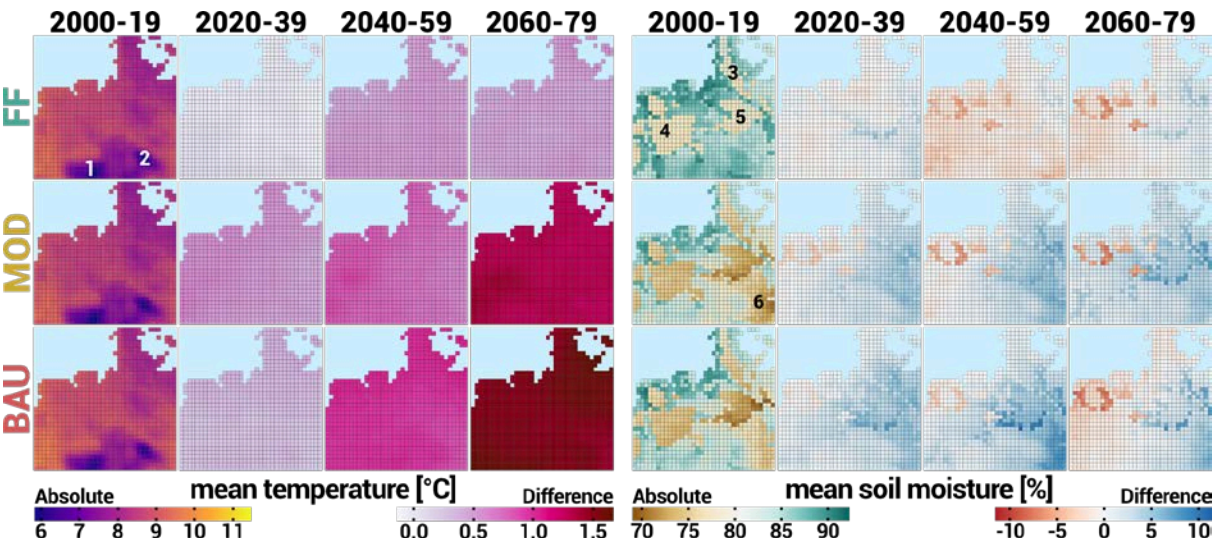

Figure 5: Spatial representation of the mean daily climate values *temperature* (LEFT) and *soil moisture* (RIGHT) for the years 2000-2079 in Northwest Germany. Within each plot, the absolute values for the simulation period 2000-19 per climate change scenario are in the first column; differences from the period 2000-19 are in the second (2020-39), third (2040-59) and fourth (2060-79) columns. The *FF* scenario is in the TOP row; the *MOD* scenario is in the MIDDLE row; the *BAU* scenario is in the BOTTOM row. Numbers mark colder mountain areas (1 and 2) and main dry regions (3-6).

On a monthly basis, the climate parameters generally followed the trends in the yearly averages (cf. Figure 3, data not shown). For all the climate change scenarios and time periods, the temperature usually reached its minimum around January and its maximum around July with gradual changes between these months. The soil moisture was lowest in September and gradually increased to its maximum in March before constantly decreasing again. An important exception from this general pattern appeared in the *BAU* scenario during the period 2060-79 (Figure 6): the monthly soil moisture values deviated from the yearly trend such that June to October were especially dry, while November to May were wetter than usual. This finding indicates a severe and possibly extended dry season that could not be detected by examining only the yearly mean values.

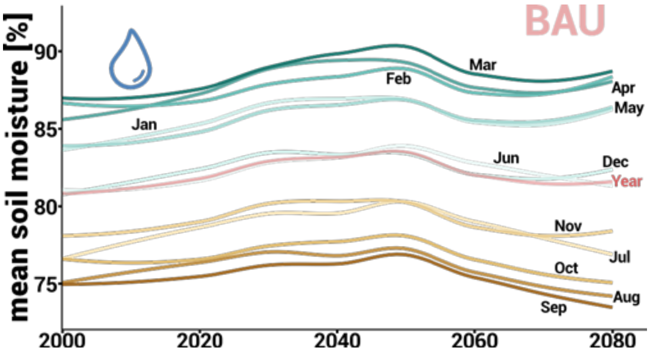

Figure 6: Projections (smoothed trends) of the mean *soil moisture* for the years 2000-2080 for the *BAU* climate change scenario distinguished by month and year (with labels).

3.2 Climate change impact on LMG

The results of the HiLEG model confirm that without direct anthropogenic influence, the LMG mostly benefits from climate change in Northwest Germany. Within each climate change scenario, there was a clear upward trend from 2000 to 2059 for both the mean density and lifetime (Figure 7). For the last simulation period (2060-79), there was a saturation yielding results similar to that of 2040-59.

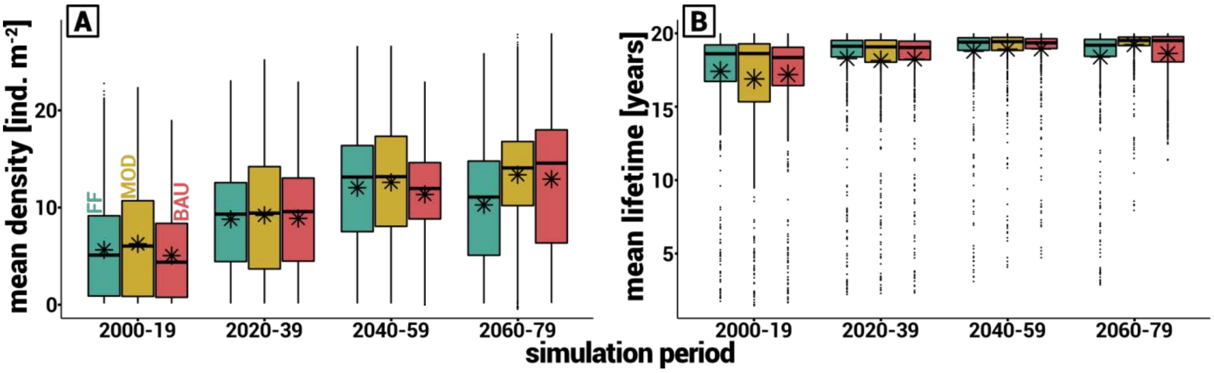

Figure 7: Population mean density [individuals m^{-2}] (A) and lifetime [years] (B) per grid cell for the study region distinguished between climate change scenarios *FF*, *MOD* and *BAU* (colored labels) and simulation periods (from left to right: 2000-19, 2020-39, 2040-59, and 2060-79). Asterisks mark the overall mean values.

Comparing the climate change scenarios within the same simulation periods, the mean results were quite similar except for differences between the *FF* scenario and the other two scenarios in the period 2060-79 (Figure 7). The scenarios led to similar spatial patterns in the mean density and lifetime within the same time period but also created certain subtle differences (Figure 8).

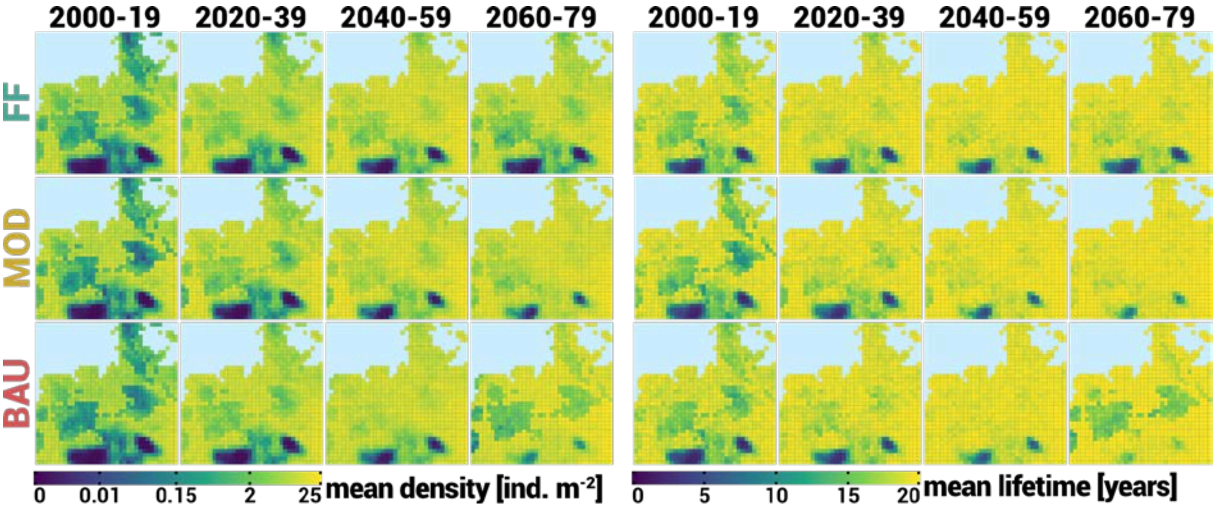

Figure 8: Log scaled mean density [individuals m^{-2}] (LEFT) and lifetime [years] (RIGHT). Within each plot the *FF*, *MOD*, *BAU* climate change scenarios are shown in the TOP, MIDDLE, and BOTTOM rows, respectively, and the simulation periods from left to right are 2000-19, 2020-39, 2040-59, and 2060-79.

First, the population conditions improved over time in initially unsuitable areas such as cold mountain regions and dry regions (cf. Figure 5, marks 1-5). An exception was 2060-79 when compared to the previous simulation period 2040-59. Here, the *FF* climate change scenario had negative effects on the mean densities and lifetimes in most of the cells. The *MOD* scenario showed almost no changes compared to the previous time period. The *BAU* scenario yielded improvements outside the dry regions but had negative effects within these dry regions.

Comparing these spatially resolved model results to the climate data showed that they reflect the temperature patterns: high temperatures support population development, while colder regions notably reduce the mean density and lifetime (Figure 5, marks 1-2). Recurrent significantly colder years (Figure 3A, 2060-79, *FF* minima) can inhibit the positive long-term effect of warm temperatures (Figure 8, 2060-79, *FF*). The soil moisture patterns, however, are less perceptible: Though population development was clearly hindered in the main dry regions (Figure 5, marks 3-5) during the simulation period 2000-19, the mean lifetime increased significantly starting in 2020. The mean density in these regions, however, remained limited compared to those in the surrounding areas. Another pattern connected to soil moisture is the strong negative effect of an extended dry season (Figure 6) on populations in most dry regions during the period 2060-79 for the *BAU* scenario (Figure 8, green areas in the bottom-right subplots).

The peaks in the mountain regions remained mostly uninhabitable for the LMG throughout all the simulations, as these areas stayed relatively cold (Figure 5, marks 1-2). In these regions, the population declined almost constantly and went extinct after a few years. This phenomenon is due to the impact of the overall lower temperatures on the LMG's development and mortality: First, it slowed down the development of the embryos and larval cohorts; second, the temperature threshold of increased larva and imago mortality occurred earlier in the year; third, the decelerated development additionally shifted larva and imago occurrence to a later, hence even colder, season of the year. Departing from the mountain peaks, the conditions for the LMG gradually improved, allowing a longer lifetime at first and increasing the population density thereafter. The time lag in population development between the warm and cold cells shown in Figure 11B (mark a) illustrates such a temperature-induced shift in the life cycle.

Low soil moisture had a negative impact on the LMG if the dry season had already started in late spring or lasted until autumn. In these cases, either the embryos (spring) or the prediapause eggs (autumn) experienced drought stress. Within the study region, extinction by drought was mainly caused by the latter, i.e., if a cell still had dry soil after oviposition (Figure 11B, mark b). Increased embryo mortality through drought stress in spring usually did not lead to extinction but minimized the mean density.

The reoccurrence of conditions unfavorable to the LMG in the period 2060-79 for the *BAU* climate change scenario was due to climate projections for this scenario. Though the notably higher temperatures led to favorable conditions in large parts of the study region, a strongly extended dry season in the central areas had considerable negative effects on the mean densities and lifetimes (Figure 8, green areas in the bottom-right subplots). As a result, the overall mean density and lifetime increased, while their larger variations (Figure 7) reflected the low values in the dry areas.

3.3 Impact of grassland mowing in addition to climate change

The extent of the negative influence of grassland mowing on the LMG life cycle was highly dependent on the calendar week in which it occurred (Figure 9). While mowing during spring and late autumn barely affected the mean lifetime, it severely reduced the mean density if it occurred in summer and early autumn. This result was independent of the climate change scenario and simulation period. However, due to the positive effect of higher temperatures in future scenarios, the time windows of negative impact both shifted and shortened: Late mowing (after week 33) became less detrimental, while early mowing (before week 26) had only a slightly more negative effect (Figure 9, *MOD* and *BAU* scenarios).

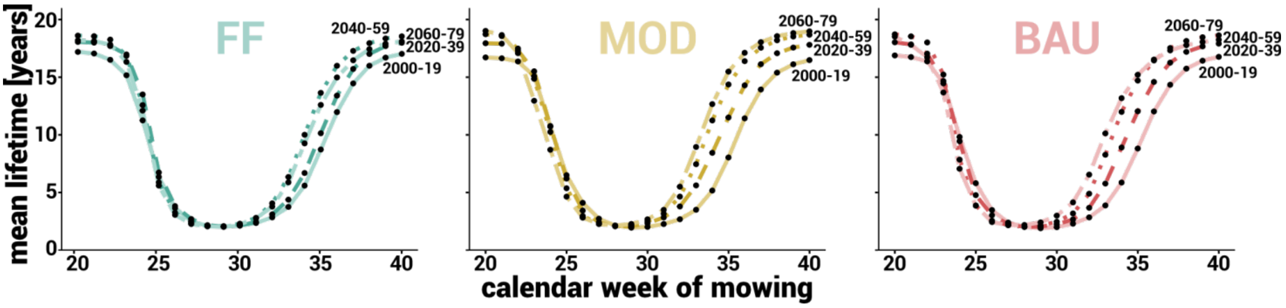

Figure 9: Population mean lifetimes averaged over the whole study region (y-axis) depending on the calendar week of grassland mowing (x-axis) for climate change scenarios *FF* (LEFT), *MOD* (MIDDLE), *BAU* (RIGHT) and the simulation periods (different line types, with labels). Mowing events (black dots) occurred on the first day of the same calendar week in each simulation year.

The spatial distribution of the mowing-dependent mean lifetime revealed regional differences between the effects of mowing timing (Figure 10). In particular, the periods of negative mowing impact did not apply to all regions in the same way. Figure 10 illustrates these differences using simulation period 2060-79 of the *BAU* climate change scenario as an example. Apart from an overall negative effect of mowing on the LMG populations (compare Figure 10B-C to Figure 10A), conditions for the LMG gradually degraded from north to south when mowing occurred early (Figure 10B). Moreover, within the southern mountain regions, the conditions remained relatively stable despite early mowing and stood out compared to their surroundings (Figure 10B). However, both patterns were inverted when mowing occurred late (Figure 10C). In this case, conditions gradually improved from north to south and were rather unsuitable within the mountain regions. Finally, as a side effect, the negative influence of mowing was generally stronger in the dry regions than in the wet regions, especially for late mowing (Figure 10C).

Note that mowing in week 23 fell into the short period of slightly more negative impact under future climate conditions than under current climate conditions (Figure 9, *BAU* scenario). Hence, the respective spatial pattern contained many cells of short mean lifetimes (dark green, Figure 10B). Nevertheless, the LMG remained rather unaffected by this scenario in the upper north and southern mountain regions. Qualitatively similar patterns were found for mowing weeks 22-26 in all three climate change scenarios and all simulation periods (see Supplement S3).

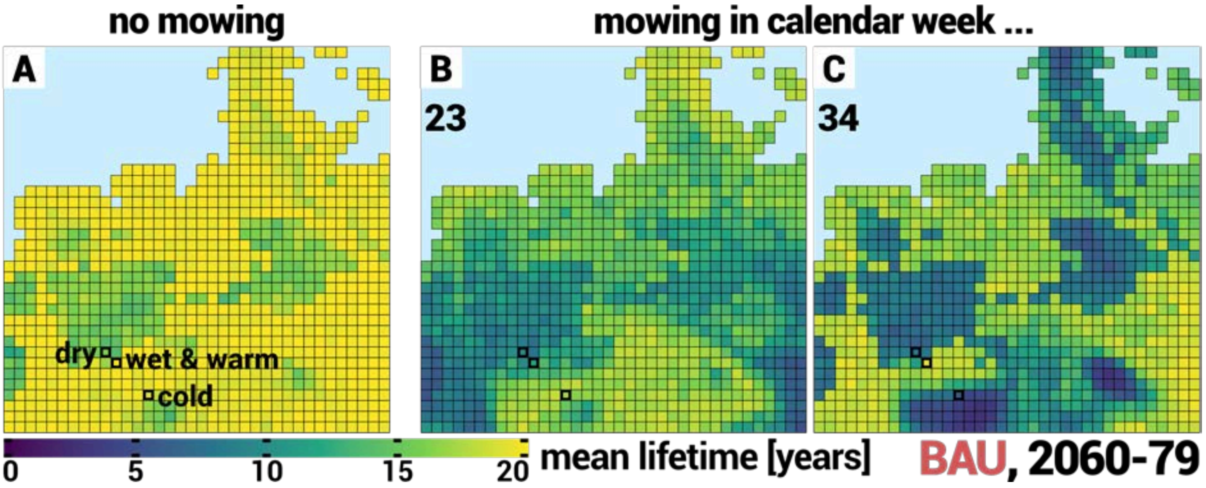

Figure 10: Spatial distributions of the mean lifetimes for the *BAU* climate change scenario and simulation period 2060-79; without mowing (A) and with mowing in calendar weeks 23 (B) or 34 (C). Thick black squares mark selected dry, wet & warm and cold cells.

The development of the mean density inside single grid cells showed that the described patterns are mainly determined by three relevant climate categories within the study region: wet and warm (mostly southern cells outside the dry and mountain regions); cold (mostly northern grid cells and especially mountain regions, Figure 5, marks 1-2); and dry (Figure 5, marks 3-5). We selected a representative grid cell for each of the climate categories (highlighted in Figure 10) to illustrate the characteristic population development (Figure 11).

The resulting population development patterns confirm that without mowing, the population eventually reached high densities in all three cell categories (Figure 11A-B). The highest values occurred under wet and warm conditions (the maximum density is already achieved in 2070), followed by cold and dry conditions. Early mowing in week 23 favored populations in cold regions but worsened the situation in dry regions; this worsening was even more prominent in wet and warm regions (Figure 11C). Late mowing in week 34 hindered population development only slightly under wet and warm conditions but hindered it more severely in dry regions (Figure 11D). Under cold conditions, late mowing had a grave impact and often caused premature extinction (Figure 11A).

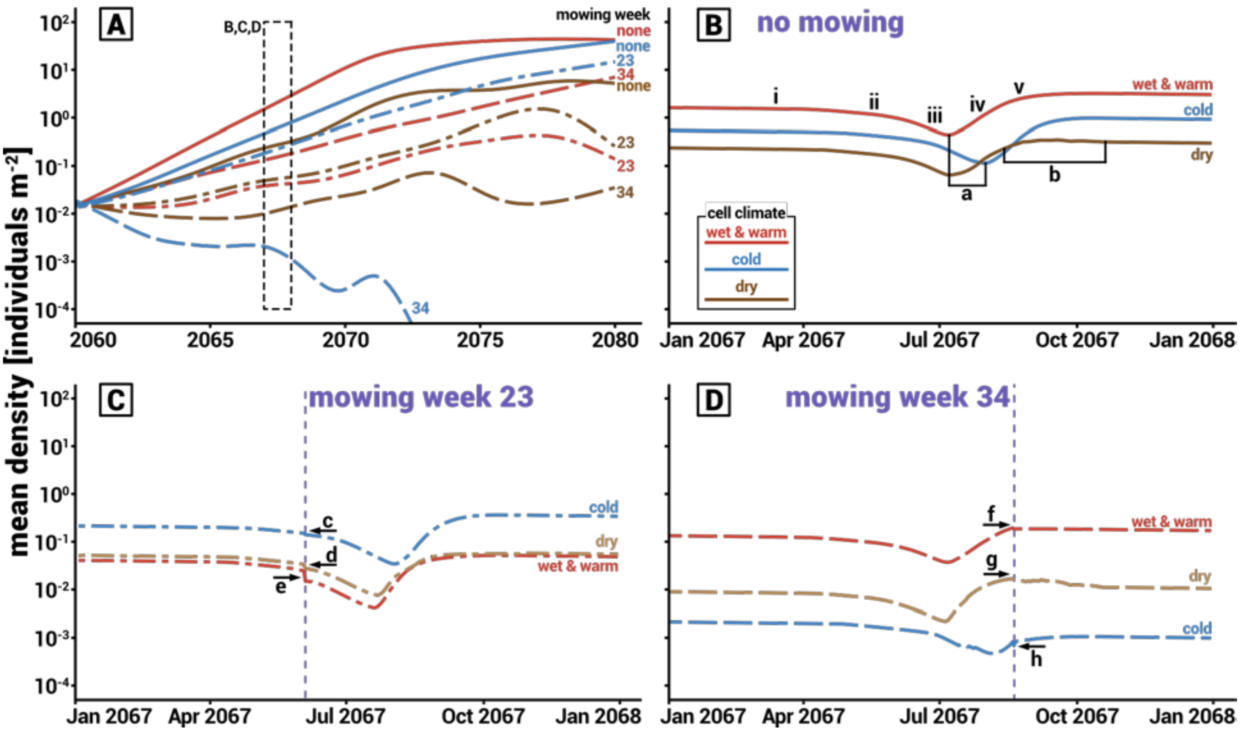

Figure 11: Trend in the mean population density (y-axis, logarithmic scale) inside three climatically different grid cells (wet & warm, red lines; cold, blue lines; dry, brown lines) without mowing (B, see also the line labels in A), with mowing in week 23 (C) and with mowing in week 34 (D) for the *BAU* climate change scenario and simulation period 2060-79. Plot A shows the smoothed trend for the whole simulation period (2060-79), and plots B-D show the detailed developments in 2067. Purple vertical lines mark the mowing weeks in C and D. Black lowercase letters (a-h) highlight the following selected events: a) shifts in the development speed, b) period of drought stress in dry cells, c) minor effect of early mowing in cold cells, d) medium effect of early mowing in dry cells, e) major effect of early mowing in wet & warm cells, f) minor effect of late mowing in wet & warm cells, g) medium effect of late mowing concurring with drought stress in dry cells, and h) major effect of late mowing in cold cells. Roman numbers in plot B indicate life stage occurrence on the basis of the development without mowing in the wet & warm cells: i) diapause, ii) embryo, iii) larva, iv) imago, v) prediapause. In plot A, the carrying capacity (25 individuals m^{-2}) is exceeded because it does not apply to the belowground population.

The main driver for the different impacts of mowing was temperature. It shifted the hatching date and altered the duration of the larval life stage. For instance, a development delay of three weeks occurred in cold cells compared to wet and warm cells (Figure 11B, mark a). This was advantageous in the case of early mowing in week 23 because – due to the delay – the population was still in the belowground phase and was thus less affected by mowing (low mortality, Figure 11C, mark c). Fast developing populations in warm cells, however, were strongly affected (Figure 11C, mark e) because many eggs had already hatched. Thus, most of the aboveground larval population was killed by mowing. In dry cells, the slightly slower population development led to a moderate loss of larvae, which prevented substantial growth (Figure 11C, mark d). These different effects of early mowing in the different cell types explain the spatial pattern in the long mean lifetimes in cold (mountain) regions and shorter lifetimes in wet and warm cells and in dry cells (Figure 10B).

In contrast, when mowing occurred later in the year, fast population development proved beneficial. In wet and warm cells, oviposition had mostly already taken place, and mowing had only a minor effect on the belowground clutch (Figure 11D, mark f). However, slowly developing populations in cold regions were hit in the middle of the aboveground phase and a large number of larvae and imagines were lost (Figure 11C, mark h). As a consequence, the small number of eggs placed in the ground resulted in a constant population reduction from year to year (Figure 11A). In dry regions, populations were affected by late mowing in week 34 (Figure 11D, mark g), which concurred during the drought period. Thus, late mowing in dry cells allowed population survival but prevented further growth (Figure 11A).

Notably, the gradients of the mean lifetime from north to south and the differences between the mountain regions and other regions (Figure 10B-C) did not occur without mowing (Figure 10A). This finding indicates that the regionally different, temperature-induced shifts in life stage development do not necessarily have considerable long-term effects on populations without mowing. However, in combination with specific mowing schedules, minor temporal shifts can have major effects on the populations' susceptibility to mowing and, thus, on long-term population development.

4 Discussion

The simulation results of the presented HiLEG model provide the following answers to our research questions: (1) outside of dry regions, climate change increases LMG population viability and promotes the species' spatial expansion; (2) grassland mowing is mostly unproblematic during autumn and winter, but highly detrimental in late spring and summer; and (3) regionally different climate conditions affect the mowing impact and should therefore be addressed by adaptive mowing schedules. These findings are discussed in more detail below.

There is basically no regional shift in the LMG distribution but an expansion in the suitable regions in Northwest Germany. The overall increasing temperatures create new potential habitats in regions that are otherwise too cold (mountainous) or too dry. This is caused either by the direct positive influence of warmth or indirectly by accelerating the LMG's development such that it suffers from drought stress less often. In fact, we found that more drastic climate change facilitates the survival and growth of the LMG even more strongly in future scenarios. The positive effects of increasing temperatures on the grasshopper's abundance and distribution visible in our results are in line with the results of Poniatowski et al. (2018) and Trautner and Hermann (2008). However, extended dry seasons, as projected for the period 2060-79 in the *BAU* climate change scenario (Figure 6), could inhibit this beneficial effect by causing drought stress for the LMG clutch. Regions affected by low soil moisture in this way (Figure 5, marks 3-5) could become less habitable for the LMG, while nearby wetter regions still benefit from the temperature increase (Figures 7 and 8, *BAU*, 2060-79). It is the duration of the dry season that makes soil moisture a crucial factor for the survival of the LMG. Although our results show that dry regions do not necessarily cause drought stress within the study region, it is likely that such a problematic extension of dry seasons will become more common in the future, especially in regions that are generally drier than Northwest Germany. Hence, at a larger scale, droughts are likely to affect the species' survival and lead to a distribution shift from dryer to wetter regions, if migration is not hindered.

Anthropogenic disturbance through land use was more critical to the viability of the species than expected climate change. The effects of grassland mowing were particularly severe when they occurred during the aboveground phase of the LMG life cycle. Currently, it is common in extensively used grasslands that the mowing season starts before the aboveground phase is reached. For instance, Gerling et al. (unpubl. results) show for the federal state of Schleswig-Holstein, a subarea of our study region, that early mowing yields the highest benefit for a farmer. Later mowing, however, has a strong impact on the LMG's development if it occurs during the aboveground phase of the population. Even when considering that imagines can partly escape harvesters (Malkus, 1997) and thus apply lower mowing-induced mortality rates (Kiel, 1999; Marzelli, 1997), the negative effect does not change qualitatively (i.e., when we reduced the imago mortality to 0.5 instead of 0.95 per day, data not shown). Although negative impacts decrease when mowing late, two counterarguments need to be considered: late mowing (after summer) is rather unprofitable for the farmer and hence may not be a feasible land use measure; and the future shift of problematic mowing to a shorter period of time in summer (Figure 9) might go along with a similar shift of vegetation growth, thus further reducing the economic profitability of late mowing.

Our simulations with the combined impact of climate change and grassland mowing revealed regional differences that need consideration when choosing a mowing schedule. The date of mowing mainly determines in which parts of the study region the impact on the species is high and where it is low. Mowing dates that are unproblematic in one region can have a highly lethal effect in another region. In most of those cases, if a population is affected by early mowing in a highly negative manner, its development is hardly influenced in simulations with late mowing. In contrast, in other regions, the population is highly disturbed by late mowing but remains mostly unaffected if mowing occurs early in the year. Altogether, the regional impact of the mowing schedule can be subdivided into five phases: (1) in early spring, the populations are largely unaffected in all regions; (2) between late spring and early summer, they are severely affected only in warm regions; (3) during summer, all populations are highly affected, barely allowing survival (Figure 9); (4) between late summer and early autumn, they are severely affected in cold regions; and (5) in autumn, populations in all regions are affected equally. The duration and beginning of each phase slightly differ between the climate change scenarios and simulation periods, but overall, they show the same pattern (see Supplement S3).

Obviously, temperature is the key factor affecting population dynamics. The LMG prefers a warm climate and hardly survives in cold (mountain) areas. That is why the simulated lifetimes are longer and population densities are higher in the more severe climate change scenarios – as long as there are no extended drought events. However, lower, not too low, temperatures can be advantageous for the LMG if early mowing is applied. As shown in Figure 11B, population development is slower in such regions, meaning that the aboveground phase, which is highly susceptible to mowing, occurs later and lasts longer. Compared to warmer regions, this finding explains the low impact during late spring and early summer (phase 2 of the phases described above) and the high negative impact during late summer and early spring (phase 4, see the examples in Figure 10B-C and Figure 11C-D)

Based on our results, we can develop some possible management strategies for a species such as the LMG to increase population viability depending on the expected climate conditions in certain regions. Our results suggest that adaptive grassland management that takes into account the local climate conditions with respect to the LMG’s life cycle would be the method of choice. In practice, however, it may prove unrealistic to implement such micromanagement. Therefore, we discuss some more generic management strategies in the following.

According to our findings, looking exclusively at climate change, the LMG mostly benefits from the projected temperature increase. Thus, the crucial parameter to consider for management strategies in such a scenario is *soil moisture*. In regions projected to experience longer dry periods, particularly if they extend into autumn, one could focus on installing, maintaining or expanding measures that keep grasslands from drying up (Miller and Gardiner, 2018), especially if those grasslands are close to streams or other fresh water bodies. Alternatively, one could consider implementing migration corridors and stepping stone biotopes to facilitate dispersal to wetter regions (Kimura and Weiss, 1964; Schumacher and Mathey, 1998). Apart from that, it is important to keep in mind that one or two carefully timed grassland cuts per year can also be considerably beneficial for the development of the LMG (Malkus, 1997). These cuts help maintain a favorable vegetation structure (Sonneck et al., 2008) and can facilitate hatching by allowing more sunlight – and, therefore, warmth – to the upper ground (Miller and Gardiner, 2018).

There are further adaptive management strategies that may allow LMG survival in cultivated grasslands. Our simulations demonstrated that intensive land use with mowing during summer, i.e., the LMG’s aboveground phase, can be lethal for a population (Figure 9). If the grassland cuts, though, are scheduled either right at the beginning or the end of the aboveground phase (Wingerden et al., 1992) or only every other year, populations can survive the cuts, though likely with low abundance. Figure 11A supports the latter suggestion by showing that populations do not immediately become extinct when exposed to a disadvantageous mowing schedule. Another possibility could be to apply different mowing schedules in neighboring grassland plots. In that way – given that individuals may migrate from one plot to another – they might find refuge until vegetation regrows (Malkus, 1997). Although those small-sized plot relations cannot be represented on the current scale of the HiLEG model, the spatial gradient covered by our model (Figure 10B-C) gives an idea of the options and necessary regional adjustments. It can make a large difference to have an offset of one or two weeks between mowing in grid cells not too far apart from each other.

In addition to adaptive scheduling, changing either the technique, e.g., inside-out-mowing (Malkus, 1997), or the mown area, e.g., by leaving uncut grass strips (Humbert et al., 2009; Kiel, 1999), could help reduce the fatalities in case the cut cannot be delayed. Uncut grass strips might even facilitate the subsequent development of the LMG because larval instars can make use of vegetation with diverse height profiles (Krause, 1996).

From a methodical point of view, our results highlight that a model's resolution can play a key role in supporting management strategies for a target species. The daily time step allowed us to capture short but distinct weather events and small seasonal shifts in the climate that would have gone unnoticed in monthly or yearly mean values. However, in our simulations, these daily dynamics had a significant impact on both short- and long-term population development. Similarly, the different impacts of environmental conditions (climate and land use) on the populations' different life stages could not have been discovered without explicitly considering the LMG life cycle and each life stage's specific characteristics. The spatial resolution of our model (12 x 12 km^2 cell^{-1}) is quite high compared to that of global climate models[4]. This high resolution allowed us to take into account spatial differences and gradients in neighboring regions, especially with regard to the suitability of mowing schedules. Szewczyk et al. (2019) state that process-based regional-scale models, such as the HiLEG model, could be further downscaled to predict species distribution at a more local or habitat level. An even higher spatial resolution could allow the consideration of additional heterogeneity in the microclimate and grassland composition of potential relevance to species such as the LMG. LMG imagines tend to choose moist locations with patchy vegetation for oviposition (Krause, 1996; Malkus, 1997). Such locations prevent drought stress (Ingrisch, 1983) and promote egg development speed, as they are sunlit (Wingerden et al., 1992). Larvae initially prefer a patchy, low- to medium-height vegetation structure (Malkus, 1997). Older instars and imagines retreat to high, dense vegetation for protection (Wingerden et al., 1992).

In this work, we intentionally consider spatial heterogeneity with regard to only the climate parameters but assume that most of the other characteristics (mowing schedule, carrying capacity, habitat size, base demographic rates) are spatially homogeneous. We make this assumption because the purpose of our analysis is to determine the impact of (spatially heterogeneous) climate change

---

[4] cf. grid resolution of global climate models: portal.enes.org/data/enes-model-data/cmip5/resolution

and its interaction with land use. The analysis would have been confounded by other sources of spatial heterogeneity. To deduce specific species conservation plans, it would be desirable and possible to include the spatial heterogeneity of the other mentioned factors as well. Another extension of the model could be to include dispersal between different grassland patches, which would allow for the migration of individuals from less suitable grassland patches to more suitable ones. Additionally, dispersal between metapopulations (Hanski, 1999; Levins, 1969) could partially provide refuge from the negative effects of grassland use through recolonization from other grassland patches (Brown and Kodric-Brown, 1977). However, Bönsel and Sonneck (2011) emphasize that metapopulation dynamics cannot be assumed for low-dispersal species such as the LMG in highly fragmented landscapes. Hence, such rescue effects will just be relevant on small spatial scales and in regions with appropriate habitat connectivity. Large-scale shifts in the spatial distribution of the species will occur only on long time scales.

5 Conclusion

We introduced the HiLEG model for the PVA of terrestrial animal species that develop through several life stages and whose development is affected by changing climate conditions and anthropogenic disturbances. The model helps identify potentially suitable regions for the species in a prospectively changing and disturbed environment. Our model can be adapted to the life cycles of different target species by setting the appropriate demographic population parameters, spatially explicit climate data and information about the timing of disturbances. In that way, it can be used as a tool for stakeholders and decision makers in conservation biology for finding strategies to conserve endangered species.

We applied our model to the LMG in Northwest Germany. The analysis showed that the LMG can broadly benefit from climate change, although with some regional variability. More importantly, however, the benefits were often not maintained in combination with land use. In particular, the timing of grassland mowing turned out to be a crucial factor for population survival. Furthermore, its effect on the species strongly depended on the spatially heterogeneous climate conditions.

Our consideration of the different population life stages and the daily resolution of the climate variables was critical for detecting unexpected, strong long-term effects on the LMG's population viability. This observation became even more prominent as the effects differed spatially.

To protect the LMG in cultivated grasslands, we suggest applying adaptive management strategies. Such strategies should consider the regional differences that mainly result from the temperature-driven development speed of LMG populations. They should be updated on a regular basis (depending on the climate change severity) to keep track of possibly changing conditions. Regions projected to experience longer and more severe dry seasons should either supply sufficiently large refugia to maintain local populations or build stepping stone habitats that allow LMG dispersal to more suitable regions. Overall, we showed that conservation of the LMG or other species with similar traits is possible even in cultivated grasslands as long as smart, adaptive and far-sighted management strategies are applied.

6 Acknowledgements

This work has been carried out within the project Ecoclimb (www.b-tu.de/en/ecoclimb), funded by the German Federal Ministry of Education and Research (grant no. 01LA1803B). We are further grateful for discussions with the other project team members and thank particularly Björn Schulz from the 'Stiftung Naturschutz Schleswig-Holstein' for providing data and literature about the large marsh grasshopper. Furthermore, we thank three anonymous reviewers for their helpful comments and suggestions.

7 References

Báldi, A., Kisbenedek, T., 1997. Orthopteran assemblages as indicators of grassland naturalness in Hungary. Agric. Ecosyst. Environ. 66, 121–129. https://doi.org/10.1016/S0167-8809(97)00068-6

Beissinger, S.R., McCullough, D.R., 2002. Population viability analysis. University of Chicago Press.

Blab, J., Nowak, E., Trautmann, W., Sukopp, H., 1984. Rote Liste der gefährdeten Tiere und Pflanzen in der BRD, erweiterte Neubearbeitung. Kilda Greven Reihe Naturschutz Aktuell 1 4.

Bonnot, T.W., 2016. Novel approaches to conserving the viability of regional wildlife populations in response to landscape and climate change (Ph. D.). University of Missouri--Columbia. https://doi.org/10.32469/10355/59821

Bönsel, A.B., Sonneck, A.-G., 2011. Habitat use and dispersal characteristic by Stethophyma grossum: the role of habitat isolation and stable habitat conditions towards low dispersal. J. Insect Conserv. 15, 455–463. https://doi.org/10.1007/s10841-010-9320-4

Brown, J.H., Kodric-Brown, A., 1977. Turnover rates in insular biogeography: effect of immigration on extinction. Ecology 58, 445–449. https://doi.org/10.2307/1935620

Chaudhary, V., Oli, M.K., 2020. A critical appraisal of population viability analysis. Conserv. Biol. 34, 26–40. https://doi.org/10.1111/cobi.13414

Cordes, L.S., Blumstein, D.T., Armitage, K.B., CaraDonna, P.J., Childs, D.Z., Gerber, B.D., Martin, J.G.A., Oli, M.K., Ozgul, A., 2020. Contrasting effects of climate change on seasonal survival of a hibernating mammal. Proc. Natl. Acad. Sci. 117, 18119–18126. https://doi.org/10.1073/pnas.1918584117

Coulson, T., Mace, G.M., Hudson, E., Possingham, H., 2001. The use and abuse of population viability analysis. Trends Ecol. Evol. 16, 219–221. https://doi.org/10.1016/S0169-5347(01)02137-1

Drechsler, M., Frank, K., Hanski, I., O'Hara, R.B., Wissel, C., 2003. Ranking metapopulation extinction risk: From patterns in data to conservation management decisions. Ecol. Appl. 13, 990–998. https://doi.org/10.1890/1051-0761(2003)13[990:RMERFP]2.0.CO;2

Green, T.W., Slone, D.H., Swain, E.D., Cherkiss, M.S., Lohmann, M., Mazzotti, F.J., Rice, K.G., 2014. Evaluating effects of everglades restoration on American crocodile populations in south Florida using a spatially-explicit, stage-based population model. Wetlands 34, 213–224. https://doi.org/10.1007/s13157-012-0370-0

Grimm, V., Berger, U., Bastiansen, F., Eliassen, S., Ginot, V., Giske, J., Goss-Custard, J., Grand, T., Heinz, S.K., Huse, G., Huth, A., Jepsen, J.U., Jørgensen, C., Mooij, W.M., Müller, B., Pe'er, G., Piou, C., Railsback, S.F., Robbins, A.M., Robbins, M.M., Rossmanith, E., Rüger, N., Strand, E., Souissi, S., Stillman, R.A., Vabø, R., Visser, U., DeAngelis, D.L., 2006. A standard protocol for describing individual-based and agent-based models. Ecol. Model. 198, 115–126. https://doi.org/10.1016/j.ecolmodel.2006.04.023

Grimm, V., Railsback, S.F., Vincenot, C.E., Berger, U., Gallagher, C., DeAngelis, D.L., Edmonds, B., Ge, J., Giske, J., Groeneveld, J., Johnston, A.S.A., Milles, A., Nabe-Nielsen, J., Polhill, J.G., Radchuk, V., Rohwäder, M.-S., Stillman, R.A., Thiele, J.C., Ayllón, D., 2020. The ODD Protocol for Describing agent-based and other simulation models: a second update to improve clarity, replication, and structural realism. J. Artif. Soc. Soc. Simul. 23, 7.

Hanski, I., 1999. Metapopulation ecology. Oxford University Press.

Helfert, B., 1980. The regulatory effect of photoperiod and temperature on the life-cycle of ecologically different tettigoniid species (Orthoptera, Saltatoria). Part 1: Larval development, reproduction and life-span of the parental generation. Zool. Jahrbucher Abt. Syst. Okologie Geogr. Tiere 107, 159–182.

Helfert, B., Sänger, K., 1975. Haltung und Zucht europäischer Heuschrecken (Orthoptera: Saltatoria) im Labor. Z. Angew. Zool.

Heydenreich, M., 1999. Die Bedeutung der Heuschreckenart Stethophyma grossum L., 1758 (Caelifera: Acrididae) als Bestandteil eines Zielartensystems für das Management von Niedermooren.

Humbert, J.-Y., Ghazoul, J., Walter, T., 2009. Meadow harvesting techniques and their impacts on field fauna. Agric. Ecosyst. Environ. 130, 1–8. https://doi.org/10.1016/j.agee.2008.11.014

Ingrisch, S., 1983. Zum Einfluß der Feuchte auf die Schlupfrate und Entwicklungsdauer der Eier mitteleuropäischer Feldheuschrecken (Orthoptera, Acrididae). Dtsch. Entomol. Z. 30, 1–15. https://doi.org/10.1002/mmnd.19830300102

Ingrisch, S., Köhler, G., 1998. Die Heuschrecken Mitteleuropas, Die Neue Brehm-Bücherei. Westarp Wissenschaften, Magdeburg.

Keller, D., Jung, E., Holderegger, R., 2012. Development of microsatellite markers for the wetland grasshopper Stethophyma grossum. Conserv. Genet. Resour. 4, 507–509. https://doi.org/10.1007/s12686-011-9586-1

Keßler, T., Cierjacks, A., Ernst, R., Dziock, F., 2012. Direct and indirect effects of ski run management on alpine Orthoptera. Biodivers. Conserv. 21, 281–296. https://doi.org/10.1007/s10531-011-0184-z

Keuler, K., Radtke, K., Kotlarski, S., Lüthi, D., 2016. Regional climate change over Europe in COSMO-CLM: Influence of emission scenario and driving global model. Meteorol. Z. 25, 121–136. https://doi.org/10.1127/metz/2016/0662

Kiel, E., 1999. Heuschrecken und Mahd. Empfehl. für Pflegemanagement Feuchtwiesenschutzgebieten–LÖBF-Mitteilungen 3, 99.

Kimura, M., Weiss, G.H., 1964. The stepping stone model of population structure and the decrease of genetic correlation with distance. Genetics 49, 561.

Kleukers, R., Van Nieukerken, E., Odé, B., Willemse, L., Van Wingerden, W., 1997. De sprinkhanen en krekels van Nederland (Orthoptera).

Köhler, G., Weipert, J., 1991. Beiträge zur Faunistik und Ökologie des Naturschutzgebietes ‘Apfelstädter Ried’, Kr Erfurt-Land Teil IV Orthoptera: Saltatoria. Arch Nat Landschaftforschung 31, 181–195.

Koschuh, A., 2004. Verbreitung, Lebensräume und Gefährdung der Sumpfschrecke Stethophyma grossum (L., 1758) (Saltatoria) in der Steiermark. Joannea Zool. 26.

Krause, S., 1996. Populationsstruktur, Habitatbindung und Mobilität der Larven von Stethophyma grossum (Linné, 1758). Articulata 11, 77–89.

Kriegbaum, H., 1988. Untersuchungen zur Lebensgeschichte von Feldheuschrecken (Orthoptera: Gomphocerinae): Fortpflanzungsverhalten und Fortpflanzungserfolg im natürlichen Habitat. PhDThesis Univ. Erlangen-Nürnberg.

Levins, R., 1969. Some demographic and genetic consequences of environmental heterogeneity for biological control. Bull. Entomol. Soc. Am. 15, 237–240. https://doi.org/10.1093/besa/15.3.237

Levy, O., Buckley, L.B., Keitt, T.H., Smith, C.D., Boateng, K.O., Kumar, D.S., Angilletta, M.J., 2015. Resolving the life cycle alters expected impacts of climate change. Proc. R. Soc. B Biol. Sci. 282, 20150837. https://doi.org/10.1098/rspb.2015.0837

Löffler, F., Poniatowski, D., Fartmann, T., 2019. Orthoptera community shifts in response to land-use and climate change – Lessons from a long-term study across different grassland habitats. Biol. Conserv. 236, 315–323. https://doi.org/10.1016/j.biocon.2019.05.058

Ma, G., Hoffmann, A.A., Ma, C.-S., 2015. Daily temperature extremes play an important role in predicting thermal effects. J. Exp. Biol. 218, 2289–2296. https://doi.org/10.1242/jeb.122127

Maas, S., Detzel, P., Staudt, A., 2002. Gefährdungsanalyse der Heuschrecken Deutschlands: Verbreitungsatlas, Gefährdungseinstufung und Schutzkonzepte; Ergebnisse aus dem F+ E-Vorhaben 89886015 des Bundesamtes für Naturschutz. na.

Malkus, J., 1997. Habitatpräferenzen und Mobilität der Sumpfschrecke (Stethophyma grossum L. 1758) unter besonderer Berücksichtigung der Mahd. Articulata 12, 1–18.

Marshall, J.A., Haes, E.C.M., 1988. Grasshoppers and allied insects of Great Britain and Ireland. Grasshopp. Allied Insects G. B. Irel.

Marzelli, M., 1997. Untersuchungen zu den Habitatansprüchen der Sumpfschrecke (Stethophyma grossum) und ihre Bedeutung für das Habitatmanagement. Articulata 12, 107–121.

McCarthy, M.A., Possingham, H.P., 2014. Population Viability Analysis, in: Wiley StatsRef: Statistics Reference Online. American Cancer Society. https://doi.org/10.1002/9781118445112.stat07746

Millennium Ecosystem Assessment, 2005. Ecosystems and human well-being: Biodiversity Synthesis. World Resour. Inst. Wash. DC 100.

Miller, J., Gardiner, T., 2018. The effects of grazing and mowing on large marsh grasshopper, Stethophyma grossum (Orthoptera: Acrididae), populations in Western Europe: a review. J. Orthoptera Res. 27(1), 91–96. https://doi.org/10.3897/jor.27.23835

Oschmann, M., 1969. Faunistisch-ökologische Untersuchungen an Orthopteren im Raum von Gotha. Hercynia - Ökol. Umw. Mitteleur. 6, 115–168.

Pe’er, G., Matsinos, Y.G., Johst, K., Franz, K.W., Turlure, C., Radchuk, V., Malinowska, A.H., Curtis, J.M.R., Naujokaitis-Lewis, I., Wintle, B.A., Henle, K., 2013. A protocol for better design, application, and communication of population viability analyses. Conserv. Biol. 27, 644–656. https://doi.org/10.1111/cobi.12076

Poniatowski, D., Münsch, T., Bianchi, F., Fartmann, T., 2018. Arealveränderungen mitteleuropäischer Heuschrecken als Folge des Klimawandels. Nat. Landsch. 553–561. https://doi.org/10.17433/12.2018.50153645.553-561

Radchuk, V., Johst, K., Groeneveld, J., Turlure, C., Grimm, V., Schtickzelle, N., 2014. Appropriate resolution in time and model structure for population viability analysis: Insights from a butterfly metapopulation. Biol. Conserv. 169, 345–354. https://doi.org/10.1016/j.biocon.2013.12.004

Radchuk, V., Turlure, C., Schtickzelle, N., 2013. Each life stage matters: the importance of assessing the response to climate change over the complete life cycle in butterflies. J. Anim. Ecol. 82, 275–285. https://doi.org/10.1111/j.1365-2656.2012.02029.x

Schmidt, N., Zinkernagel, J., 2017. Model and growth stage based variability of the irrigation demand of onion crops with predicted climate change. Water 9, 693. https://doi.org/10.3390/w9090693

Schumacher, U., Mathey, J., 1998. Zur Analyse der Lebensräume von Heuschrecken mit Methoden der Geoinformatik-dargestellt am Beispiel der Riesaer Elberegion, in: Angewandte Geographische Informationsverarbeitung. Beiträge Zum AGIT-Symposium Salzburg.

Sonneck, A.-G., Bönsel, A., Matthes, J., 2008. Der Einfluss von Landnutzung auf die Habitate von Stethophyma grossum (Linnaeus, 1758) an Beispielen aus Mecklenburg-Vorpommern. Articulata 23, 15–30.

Stephens, P., 2016. Population viability analysis. Oxford University Press.

Szewczyk, T.M., Lee, T., Ducey, M.J., Aiello-Lammens, M.E., Bibaud, H., Allen, J.M., 2019. Local management in a regional context: Simulations with process-based species distribution models. Ecol. Model. 413, 108827. https://doi.org/10.1016/j.ecolmodel.2019.108827

Thompson, L.C., Escobar, M.I., Mosser, C.M., Purkey, D.R., Yates, D., Moyle, P.B., 2012. Water management adaptations to prevent loss of spring-run Chinook salmon in California under climate change. J. Water Resour. Plan. Manag. 138, 465–478. https://doi.org/10.1061/(ASCE)WR.1943-5452.0000194

Trautner, J., Hermann, G., 2008. Die Sumpfschrecke (Stethophyma grossum L., 1758) im Aufwind-Erkenntnisse aus dem zentralen Baden-Württemberg. Articulata 23, 37–52.

Uvarov, B., 1977. Grasshoppers and locusts. A handbook of general acridology Vol. 2. Behaviour, ecology, biogeography, population dynamics. Grasshopp. Locusts Handb. Gen. Acridology Vol 2 Behav. Ecol. Biogeogr. Popul. Dyn.

van Vuuren, D.P., Edmonds, J., Kainuma, M., Riahi, K., Thomson, A., Hibbard, K., Hurtt, G.C., Kram, T., Krey, V., Lamarque, J.-F., Masui, T., Meinshausen, M., Nakicenovic, N., Smith, S.J., Rose, S.K., 2011. The representative concentration pathways: an overview. Clim. Change 109, 5. https://doi.org/10.1007/s10584-011-0148-z

Waloff, N., 1950. The egg pods of British short-horned grasshoppers (acrididae). Proc. R. Entomol. Soc. Lond. Ser. Gen. Entomol. 25, 115–126. https://doi.org/10.1111/j.1365-3032.1950.tb00088.x

Wingerden, W.K.R.E. van, Musters, J.C., Cannemeijer, F., Bongers, W., 1992. Simulation of hatching date in three Chorthippus species (Orthoptera arcrididae) in unfertilized and lightly fertilized grasslands.

Wingerden, W.K.R.E. van, Musters, J.C.M., Maaskamp, F.I.M., 1991. The influence of temperature on the duration of egg development in West European grasshoppers (Orthoptera: Acrididae). Oecologia 87, 417–423. https://doi.org/10.1007/BF00634600

Winkler, C., 2000. Die Heuschrecken Schleswig-Holsteins - Rote Liste, Rote Liste [Schleswig-Holstein]. Eigenverl, Flintbek.